casian and African Americans. The six haplotypes occur in 21 different genotypes that were tested versus other haplotype genotype combinations for progression rate to AIDS using the CDC case definition of AIDS from 1993 (*22*). We also tested separate and combined cohorts for the various genotypes effect on AIDS progression using the more stringent 1987 AIDS definition (*22*). In African Americans, all of the promoter allele genotypes were considered in Cox analyses, of which none were significant. Bonferroni corrections for multiple tests were performed as described [B. S. Weir, *Genetic Data Analysis* (Sinauer, Sunderland, MA, 1990); T. Schweder and E. Spjotvoll, *Biometrika* **69**, 493 (1982)].

21. The AIDS protective effects of the three genotypes *CCR5-+/Δ32*, *CCR2-+/64I*, and *SDF1-3′A/3′A* observed in the same cohorts (*1, 5–11, 16*) was used to quantitatively weight their influence on AIDS progression by considering these as covariables in the Cox analysis of *CCR5P* genotypes. The *CCR5* and *CCR2* effects have been confirmed in multiple studies (*8, 10, 11*), whereas the *SDF1* protection has been affirmed for the death endpoint in one study (*33*) but not in another (*24*). We have chosen to consider *SDF1-3′A/3′A* as protective because that is the observation for the cohorts considered here in both separate and combined analyses.
22. U.S. Centers for Disease Control and Prevention, 1993 revised classification system for HIV infection and expanded surveillance case definition for AIDS among adolescents and adults [*Morb. Mortal. Wkly. Rep.* **41**, 1 (1992)]; U.S. Centers for Disease Control, classification system for HIV-1 infection [*ibid.* **36** (suppl. 1) (1987)].
23. P. D. Allison, *Survival Analyses Using the SAS System: A Practical Guide* (SAS Institute, Cary, NC, 1995), pp. 155–157.
24. S. Mummidi *et al.*, *Nature Med.* **4**, 786 (1998).
25. D. Littman, *Cell* **93**, 677 (1998).
26. L. Wu *et al.*, *J. Exp. Med.* **185**, 1681 (1997).
27. M. Benkirane *et al.*, *J. Biol. Chem.* **272**, 30603 (1997).
28. Quantitative fluorescence-activated cell sorting (FACS) analysis was done on various subsets of PBMCs. Four-color FACS was used to quantify the amount of 2D7 binding sites on fresh, unstimulated $CD4^+$ memory and naïve T cells from individuals wild-type for the *CCR5* and *CCR2 ORF* locus. CCR5 was not expressed on naïve T cells ($CD45RO^-$) but was present on memory T cells ($CD45RO^+$). Among memory T cells, relative to the $CD62L^+$ subset, the $CD62L^-$ subset (true memory cells) expressed at least five times as much CCR5 on the cell surface. This was true regardless of the *CCR5* promoter genotype.
29. A. McMichael, *Cell* **93**, 673 (1998).
30. M. L. Levin, *Acta Unio Int. Contra Cancrum* **9**, 531 (1953); M. J. Khoury, T. H. Beaty, B. H. Cohen, *Fundamentals of Genetic Epidemiology. Monographs in Epidemiology and Biostatistics* (Oxford Univ. Press, New York, 1993).
31. J. P. A. Ionnidis *et al.*, *Nature Med.* **4**, 536 (1998).
32. M. Carrington *et al.*, in preparation.
33. R. P. Van Rij *et al.*, *AIDS* **12**, F85 (1998).
34. D. H. McDermott *et al.*, *Lancet* **352**, 866 (1998).
35. S. M. Donfield, H. S. Lynn, M. W. Hilgartner, *Science* **280**, 1819 (1998); W. Smith *et al.*, *ibid.*, p. 1820; M. W. Smith, *Nature Med.* **3**, 1052 (1997).
36. The possibility that the AIDS acceleration effects associated with the [+.*P1*.+]/[+.*P1*.+] genotype might reflect differences in survival due to better treatments late in the epidemic is unlikely because the clinical data used here were collected from 1978 to 1996, before the wide use of highly active antiretroviral therapy (HAART). Further, the distribution of *CCR5P1/P1* accelerating genotypes was examined in different time periods of the AIDS epidemic with our patients as follows. Three Caucasian groups (combined cohort seroconverters, $N = 632$; MACS seroconverters, $N = 397$; and MHCS seroconverters, $N = 226$) were partitioned into halves and thirds on the basis of date of seroconversion. We observed a modest depletion of [+.*P1*.+]/[+.*P1*.+] homozygotes in the earlier seroconverters (9% vs. 15% in later groups; $P = 0.01$ to 0.14) in six separate tests. In addition, [+.*P1*.+]/[+.*P1*.+] seroconverters infected early survived longer than those infected later. Both of these results likely reflect depletion of the most rapid progressors from certain categories, particularly hemophiliacs, plus the higher failure rates for Epstein-Barr virus transformation (providing DNA) among rapid progressors (*35*). If affirmed, the increase of protective [+.*P1*.+]/[+.*P1*.+] genotypes in later seroconverters and the longer survival of early versus late [+.*P1*.+]/[+.*P1*.+] patients are inconsistent (in the wrong direction) with a scenario whereby more effective recent therapies influenced the genetic effects. Pre-1996 treatment with AZT (zidovudine) was not considered formally because timing, duration, and dosage were sporadic in these patients, precluding a robust analysis.
37. Supported by the National Cancer Institute of NIH under contract N01-CO-56000.

15 July 1998; accepted 28 October 1998

Role of MEKK1 in Cell Survival and Activation of JNK and ERK Pathways Defined by Targeted Gene Disruption

Toshiaki Yujiri, Susan Sather, Gary R. Fanger, Gary L. Johnson*

Targeted disruption of the gene encoding MEK kinase 1 (MEKK1), a mitogen-activated protein kinase (MAPK) kinase kinase, defined its function in the regulation of MAPK pathways and cell survival. $MEKK1^{-/-}$ embryonic stem cells from mice had lost or altered responses of the c-Jun amino-terminal kinase (JNK) to microtubule disruption and cold stress but activated JNK normally in response to heat shock, anisomycin, and ultraviolet irradiation. Activation of JNK was lost and that of extracellular signal-regulated protein kinase (ERK) was diminished in response to hyperosmolarity and serum factors in $MEKK1^{-/-}$ cells. Loss of MEKK1 expression resulted in a greater apoptotic response of cells to hyperosmolarity and microtubule disruption. When activated by specific stresses that alter cell shape and the cytoskeleton, MEKK1 signals to protect cells from apoptosis.

MEKK1 is a 196-kD protein serine-threonine kinase that has regulatory sequences for binding the small guanine nucleotide–binding proteins Ras (*1*) and Cdc42/Rac (*2*), an NH_2-terminal bidentate 14-3-3 binding site (*3*), and a putative pleckstrin homology domain. When transfected into various cell types, MEKK1 activates the JNK and ERK pathways (*4, 5*). Expression of the catalytic domain of MEKK1 preferentially activates the JNK pathway (*5*). In contrast, expression of the complete enzyme effectively activates both the JNK and ERK pathways (*6*). MEKK1 is activated through the epidermal growth factor (EGF) receptor in PC12 (*7*), Cos (*3*), and T47D cells (*8*); the formyl-Met-Leu-Phe receptor in neutrophils (*9*); and antigen ligation of the high-affinity immunoglobulin E receptor, FcεR1, in mast cells (*10*). Catalytically inactive inhibitory mutants of MEKK1 block receptor activation of both the JNK and ERK pathways (*2*), suggesting MEKK1 has the potential to regulate both MAPK pathways. MEKK1 is also a caspase-3 substrate (*11*). Cleavage of MEKK1 at Asp^{874} releases from cell membranes a 91-kD COOH-terminal kinase domain that amplifies caspase activation and induces apoptosis (*11*).

In mammalian cells, it is unprecedented for a MAPK kinase kinase to regulate two MAPK

Program in Molecular Signal Transduction, Division of Basic Sciences, National Jewish Medical and Research Center, Denver, CO 80206, USA, and the Department of Pharmacology, University of Colorado Medical School, Denver, CO 80262, USA.

*To whom correspondence should be addressed. E-mail: johnsong@njc.org

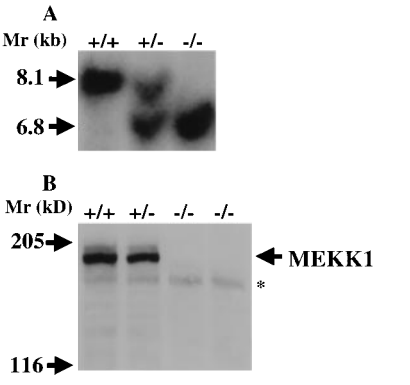

Fig. 1. Gene targeting of MEKK1. (**A**) Genomic analysis of ES cells. Genomic DNA was isolated from $MEKK1^{+/+}$, $MEKK^{+/-}$, and $MEKK1^{-/-}$ cells, digested with Eco R1, and analyzed by Southern blotting with a 5′ flanking probe. (**B**) Absence of MEKK1 protein in $MEKK1^{-/-}$ cells. Cell lysates from $MEKK1^{+/+}$, $MEKK1^{+/-}$, and $MEKK1^{-/-}$ cells were resolved by SDS-PAGE, transferred to filters, and probed with an antibody to the COOH-terminus of MEKK1. The faint band (*) is a nonspecific band that is not related to MEKK1. Four additional antisera to different MEKK1 epitopes did not detect this band in MEKK1 immunoblots. Mr, molecular mass.

pathways in response to different extracellular stimuli. To define the specific stimuli that require the 196-kD MEKK1 for activation of specific MAPK pathways, we generated mouse embryonic stem (ES) cell lines lacking MEKK1 expression by homologous recombination (Fig. 1A) (*12*). Mutation of both MEKK1 alleles ($MEKK1^{-/-}$) was established by selection in a high concentration of G418. Expression of the 196-kD MEKK1 protein was diminished in $MEKK1^{+/-}$ cells and absent in $MEKK1^{-/-}$ cells (Fig. 1B). The expression of Raf-1, B-Raf, ERK, JNK, and p38 proteins was unchanged in $MEKK1^{-/-}$ cells (*13*).

MEKK1 is a strong activator of the JNK pathway (*2, 5*). However, the stress response pathways that require MEKK1 are not defined. To define the role of MEKK1 in activation of the JNK pathway by different extracellular inputs, we exposed $MEKK1^{-/-}$ and $MEKK1^{+/+}$ cells to several different stress stimuli, including microtubule disruption by nocodazole, cold shock, hyperosmolarity, ultraviolet (UV) irradiation, anisomycin, and heat shock (Fig. 2, A to D) (*14*). In addition, $MEKK1^{-/-}$ and $MEKK1^{+/+}$ cells were deprived of serum for 2 hours and then stimulated with fetal bovine serum (FBS) (15%) (Fig. 2E) or lysophosphatidic acid (LPA) (Fig. 2F). The results revealed a distinct selectivity for participation of MEKK1 in activating JNK in response to various stimuli. MEKK1 was not required for JNK activation in response to UV irradiation, anisomycin, or heat shock (Fig. 2A). MEKK1 was required for JNK activation in response to microtubule disruption by nocodazole (Fig. 2B) and cold shock (Fig. 2C). MEKK1 was also required for JNK activation in response to modest hyperosmolarity achieved by the addition of sorbitol at concentrations up to 200 mM to the growth medium (Fig. 2D). Sorbitol concentrations above 200 mM resulted in the activation of the JNK pathway in both $MEKK1^{-/-}$ and $MEKK^{+/+}$ cells. This finding indicates that two mechanisms exist in ES cells to respond to hyperosmolarity and that only one requires MEKK1. Activation of the JNK pathway by serum factors evident in $MEKK1^{+/+}$ cells was virtually absent in $MEKK1^{-/-}$ cells (Fig. 2E). The serum response was mimicked by LPA (Fig. 2F), indicating that MEKK1 is required for JNK activation by the primary mitogen in serum.

Table 1 summarizes results from three to eight independent experiments with two $MEKK1^{-/-}$ clones. The results show that basal JNK activity is significantly diminished in $MEKK1^{-/-}$ cells. Furthermore, the stimulation of JNK activity in response to serum, LPA, nocodazole, low-dose sorbitol, and cold stress is markedly blunted. In contrast, the JNK stimulation in response to heat shock, anisomysin, and UV irradiation is similar in wild-type and two $MEKK1^{-/-}$ clones.

Direct measurement of MEKK1 activity, assessed by its ability to phosphorylate recombinant MKK4 (also referred to as SEK1) (*15*), a MAPK kinase in the JNK pathway (*16*), confirmed that MEKK1 was activated in response to nocodazole, cold temperature, sorbitol, and serum (Fig. 3). MEKK1 also showed a shift to a slower mobility during SDS–polyacrylamide gel electrophoresis (SDS-PAGE) when isolated from $MEKK1^{+/+}$ cells exposed to sorbitol. The

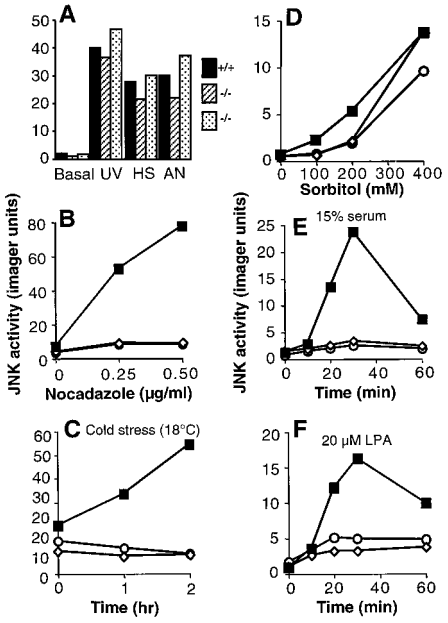

Fig. 2. Stimulation of JNK in $MEKK1^{+/+}$ and $MEKK1^{-/-}$ cells. JNK activation was measured in response to (**A**) UV irradiation (100 J/m^2), 42°C heat shock (HS) for 30 min, or anisomycin (AN) (50 ng/ml) for 30 min, (**B**) two concentrations of nocodazole for 1 hour, (**C**) cold stress induced by incubation at 18°C, (**D**) various concentrations of sorbitol for 30 min, (**E**) various times with 15% FBS, and (**F**) various times with 20 μM LPA. The results are for $MEKK1^{+/+}$ cells (squares) and two independent $MEKK1^{-/-}$ clones (circles and diamonds). Shown is one experiment that is representative of three to seven experiments for the different clones and conditions.

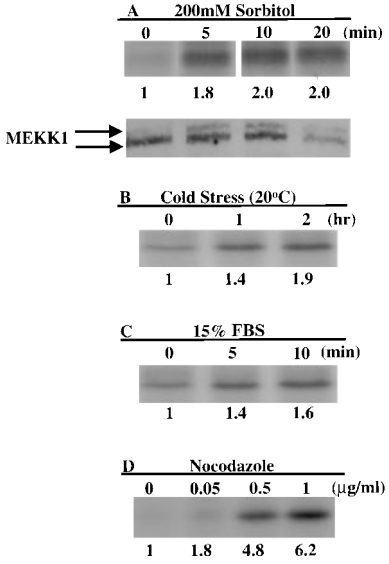

Fig. 3. Activation of MEKK1 in $MEKK1^{+/+}$ cells. Wild-type ES cells were (**A**) treated with 200 mM sorbitol for the indicated times, (**B**) treated with cold stress (20°C) for 1 and 2 hours, (**C**) deprived of FBS and leukemia inhibitory factor for 2 hours and then treated for 5 or 10 min with FBS (15%), or (**D**) incubated with nocodazole (0.05, 0.5, or 1 μg/ml) for 1 hour. MEKK1 activity was assayed in immunoprecipitates with recombinant catalytically inactive MKK4 as substrate. Fold activation over basal MEKK1 activity was determined by phosphorimaging and is shown below each lane. In (A), MEKK1 was resolved by SDS-PAGE, transferred to a filter, and immunoblotted (bottom panel).

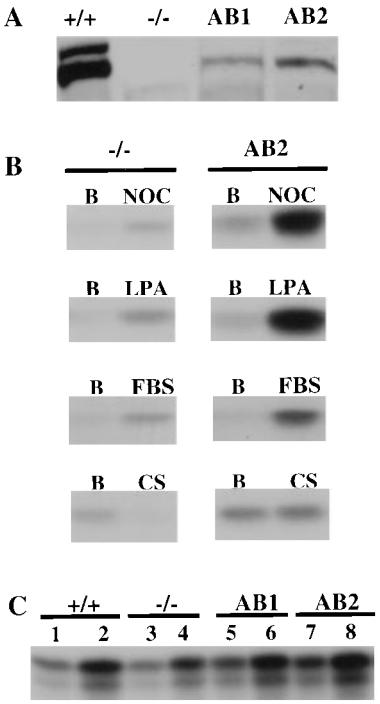

Fig. 4. Restoration of the JNK and ERK response by expression of MEKK1 in $MEKK1^{-/-}$ cells. $MEKK1^{-/-}$ cells ($-/-$) were stably transfected with the cDNA for full-length MEKK1 in the expression plasmid pCEP4 and selected for resistance to hygromycin. (**A**) Clones expressing MEKK1 (AB1 and AB2) were identified by immunoblotting. (**B**) Expression of MEKK1 restored JNK activation in response to nocodazole (NOC; 0.5 μg/ml), 1 μM LPA, 15% FBS, and cold shock at 20°C (CS) relative to unstimulated cells having a basal (B) JNK activity. (**C**) Cells were serum starved for 2 hours and then challenged with 15% FBS for 10 min. ERK activity was measured after cell lysis and immunoprecipitation by phosphorylation of myelin basic protein. FBS-stimulated ERK activity in AB1 and AB2 was similar to that for the wild-type $+/+$ ES cells. MEKK1 add-back clones (AB1 and AB2) had a higher basal ERK activity relative to $-/-$ clones. FBS-stimulated ERK activity is diminished in $-/-$ cells. Basal activity, lanes 1, 3, 5, and 7; serum stimulation, lanes 2, 4, 6, and 8.

gel shift is related to MEKK1 phosphorylation and activation (*11*). Thus, MEKK1 is activated and required for stimulation of the JNK pathway in response to microtubule disruption, mild hyperosmolarity, cold stress, or serum factors, including LPA. Activation of the JNK pathway in response to other stress stimuli, including UV irradiation, anisomycin, and heat shock, did not require MEKK1. Evidently, other MAPK kinase kinases must respond to these stress stimuli and activate the JNK pathway.

The loss of JNK regulation by specific stimuli was demonstrated to directly result from the loss of MEKK1 expression. MEKK1$^{-/-}$ cells were stably transfected with the MEKK1 cDNA, and clones were screened for expression of the 196-kD enzyme. Two independent transfected MEKK1$^{-/-}$ clones that express MEKK1 driven by the cytomegalovirus promoter from the pCEP4 expression plasmid are shown in Fig. 4A. Higher levels of MEKK1 expression could not be obtained. We observed the cell cycle–dependent regulation of endogenous MEKK1 expression that is not mimicked when it is constitutively expressed from a plasmid (*13*). Nonetheless, add-back of MEKK1 at the expression levels achieved reconstituted the JNK response to nocodazole, LPA, and serum (Fig. 4B). In addition, cold stress inhibits JNK activity in MEKK1$^{-/-}$ cells, which is prevented by the add-back of MEKK1 expression, consistent with MEKK1 being required for JNK regulation during cold stress.

When overexpressed, MEKK1 activates the ERK and JNK pathways (*2, 4, 5*). In vitro, MEKK1 phosphorylates and activates MKK1 (also referred to as MEK1), the MAPK kinase in the ERK pathway (*4*). Furthermore, catalytically inactive MEKK1 inhibits stimulation of ERK in response to EGF (*2*). ERK activity was modest in ES cells (*17*). Two-hour serum deprivation was observed to significantly diminish basal ERK activity in MEKK1$^{-/-}$ cells but not in wild-type ES cells (Table 1). ERK stimulation by sorbitol, serum, and LPA but not phorbol ester was also diminished in MEKK1$^{-/-}$ clones. These results, statistically analyzed for multiple independent experiments, show that MEKK1 contributes to ERK activation. However, the contribution of MEKK1 to ERK activation in response to different stimuli is only partial, because of the overlapping activation of Raf-1 and B-Raf, which also activate ERK. Expression of MEKK1 by stable transfection of the MEKK1$^{-/-}$ ES cells restored ERK activation in response to serum factors (Fig. 4C). Basal and serum-stimulated ERK activity was elevated in the add-back clones relative to MEKK1$^{-/-}$ cells, demonstrating that MEKK1 contributes to regulation of the ERK pathway in addition to the JNK pathway. Activation of p38 in response to hyperosmolarity was identical in MEKK$^{-/-}$ and MEKK$^{+/+}$ cells (Table 1). MEKK1 does not appear to regulate p38.

Our results indicate that MEKK1 is a MAPK kinase kinase that selectively regulates two different MAPK modules. In *Saccharomyces cerevisiae*, the MAPK kinase kinase STE11 participates in MAPK pathways functioning in pheromone-regulated mating, pseudohyphal or invasive growth, and hyperosmolarity (*18*). The MAPK kinase for mating and pseudohyphal or invasive growth is STE7, whereas the MAPK differs: Fus 3 for mating and KSS1 for pseudohyphal or invasive growth. In the hyperosmotic response

Table 1. Regulation of JNK, ERK, and p38 activity in wild-type and MEKK1$^{-/-}$ ES clones. JNK, ERK, and p38 activity data from three to eight experiments were pooled and statistically analyzed for each stimulus for wild-type (+/+) and two MEKK1$^{-/-}$ (−/−) ES cell clones. Values were determined by phosphorimager analysis, where basal activity was given a value of 1. Fold stimulation was then analyzed for each stimulus. Data are presented as the mean ± SEM. Where SEM is not shown, the data are the mean of two experiments. Incubation times for each stimulus were 10 and 30 min for ERK and p38, respectively. For JNK activation, incubation times varied: FBS, LPA, sorbitol, heat shock, and anisomycin, 30 min; nocodazole, 1 hour; cold shock, 2 hours; and UV, 1 hour after irradiation.

Condition	+/+	−/−	−/−
	JNK activity		
Basal (+ serum)	1.0	0.6 ± 0.2*	0.6 ± 0.2*
+15% FBS (2 hours starvation)	15 ± 3.0	2.3 ± 0.1*	3.7
LPA (20 μM)	22 ± 4	3 ± 0.9*	4.5 ± 1.6*
Nocodazole (0.5 μg/ml)	6.9 ± 2.1	1.6 ± 0.4*	2.2 ± 0.3*
Sorbitol			
100 mM	3.5 ± 1.7	1.6 ± 0.6*	1.5
200 mM	7 ± 2	3.9 ± 0.3*	3.8
400 mM	21 ± 11	25 ± 7	19 ± 5
Cold shock (18°C)	2.0 ± 0.5	0.6 ± 0.2*	0.6
Heat shock (42°C)	20 ± 6	16 ± 11	30 ± 12
Anisomycin (10 μg/ml)	20 ± 9	19 ± 10	28 ± 6
UV (100 J/m^2)	27 ± 10	28 ± 9	29 ± 6
	ERK activity		
Basal (+ serum)	1.0	0.9 ± 0.1	1.1 ± 0.1
2 hours serum starvation	1.0	0.7 ± 0.1*	0.7 ± 0.2*
Sorbitol (200 mM)	2.8 ± 0.4	1.7 ± 0.4*	1.8 ± 0.2*
15% FBS	3.9 ± 0.2	1.8	1.4 ± 0.1*
LPA (20 μM)	2.7 ± 0.5	2.0 ± 0.3*	—
PMA (100 nM)	3.4 ± 1.5	3.3 ± 1.4	2.8 ± 0.5
	p38 activity		
Sorbitol			
100 mM	1.4 ± 0.05	1.2 ± 0.1	1.4 ± 0.2
200 mM	3.3 ± 1.3	2.4 ± 0.6	3.4 ± 0.1
400 mM	7.7 ± 4.6	6.0 ± 2.4	6.4 ± 1.6

* A significant difference at a P value of 0.05 with the Student's t test.

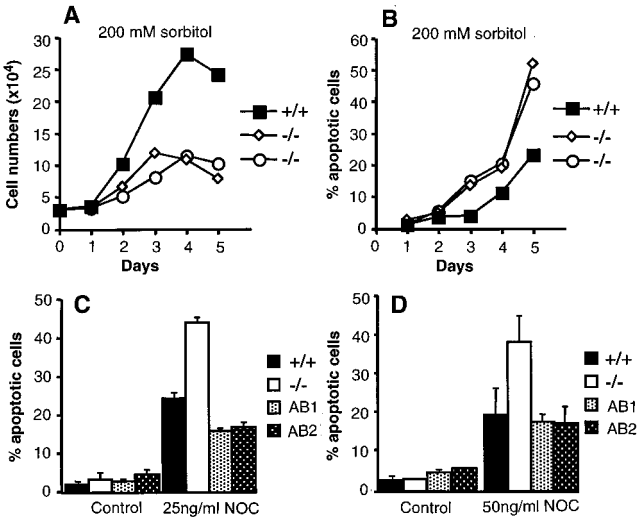

Fig. 5. MEKK1$^{-/-}$ cells have an increased apoptotic response to stress. (**A** and **B**) MEKK1$^{+/+}$ and MEKK1$^{-/-}$ cells were grown in the presence of 200 mM sorbitol. Cell numbers were determined on days 1 to 5. The growth of −/− cells is substantially less than that of +/+ cells in the presence of sorbitol. Contributing to the decreased cell number for −/− clones is an increased apoptotic rate. (**C** and **D**) Nocodazole (NOC) treatment of ES cells disrupts microtubules and induces apoptosis. MEKK1$^{-/-}$ cells are more sensitive to nocodazole as measured by percentage of apoptotic cells 16 hours after exposure to drug. The add-back of MEKK1 expression (AB1 and AB2) rescued the −/− ES cells so that their sensitivity to nocodazole-induced apoptosis was similar to +/+ cells. Shown are two independent experiments where values represent the mean of triplicate samples ± SEM. Apoptosis was measured by acridine orange–ethidium bromide staining and also verified by terminal deoxytransferase analysis of DNA fragmentation for sorbitol treatment (*13*).

pathway, the MAPK kinase and MAPK are Pbs2 and Hog1, respectively (*18, 19*). We found that, like STE11, MEKK1 responds to different stimuli for the selective regulation of at least two MAPK pathways.

Nocodazole treatment of cells did not significantly activate ERK (*13*). Thus, MEKK1 activation in response to microtubule disruption selectively stimulates JNK. Nocodazole, cold stress, and mild hyperosmolarity all require MEKK1 for JNK activation. The common feature of each of these stresses is a cell shape change, suggesting that MEKK1 activates JNK in response to sensors that detect shape changes. MEKK1$^{-/-}$ cells have a diminished capacity to survive stresses including mild hyperosmolarity and nocodazole-induced disruption of microtubules (Fig. 5). Thus, MEKK1 is required for survival during environmental challenges that stress cells. In normal medium, the growth of MEKK1$^{-/-}$ and wild-type ES cells is similar. Treatment of ES cells with sorbitol inhibited the growth of MEKK1$^{-/-}$ cells relative to wild-type ES cells (Fig. 5A). In addition to sorbitol-induced growth arrest, the number of apoptotic cells was substantially greater for MEKK1$^{-/-}$ compared with wild-type ES cells (Fig. 5B). MEKK1$^{-/-}$ cells were also substantially more sensitive to nocodazole-induced apoptosis (Fig. 5, C and D). MEKK1 expression in transfected MEKK1$^{-/-}$ clones restored the survival response to that of wild-type ES cells just as it reconstituted JNK activation in response to nocodazole treatment.

The antiapoptotic function of MEKK1 activation has been defined by its targeted disruption. The findings define the ability of MEKK1 to enhance the survival of cells after a stress response. MEKK1 promotion of cell survival is opposite to its described proapoptotic function initiated when it is cleaved by caspases (*11*). Caspase cleavage of MEKK1 releases a 91-kD activated kinase domain that further amplifies caspase activity committing cells to apoptosis; activated full-length 196-kD MEKK1 activates neither caspases nor apoptosis (*20*). Thus, there is a dual role for MEKK1 controlled by its cleavage. Caspases act as switches to convert the MEKK1 survival signal to a proapoptotic response.

References and Notes

1. M. Russell, C. A. Lange-Carter, G. L. Johnson, *J. Biol. Chem.* **270**, 11757 (1995).
2. G. R. Fanger, N. L. Johnson, G. L. Johnson, *EMBO J.* **16**, 4961 (1997).
3. G. R. Fanger *et al*., *J. Biol. Chem.* **273**, 3476 (1998).
4. C. A. Lange-Carter, C. M. Pleiman, A. M. Gardner, K. J. Blumer, G. L. Johnson, *Science* **260**, 315 (1993).
5. A. Minden, A. Lin, F. Claret, A. Abo, M. Karin, *Cell* **81**, 1147 (1995).
6. C. Widmann and G. L. Johnson, unpublished data.
7. C. A. Lange-Carter and G. L. Johnson, *Science* **265**, 1458 (1994).
8. G. R. Fanger and G. L. Johnson, unpublished data.
9. N. J. Avdi *et al*., *J. Biol. Chem.* **271**, 33598 (1996).
10. T. Ishizuka *et al*., *ibid*., p. 12762.
11. C. Widmann, P. Gerwins, N. L. Johnson, M. B. Jarpe, G. L. Johnson, *Mol. Cell. Biol.* **18**, 2416 (1998).
12. Genomic DNA clones corresponding to the MEKK1 locus were cloned from a λ FixII phage library prepared from mouse strain 129/sv (Stratagene). The targeting vector was constructed by inserting a 3.8-kb Bam H1–Bam H1 fragment from the 5′ end of the genomic clone into the Sal 1 site of the targeting vector. A 2.0-kb Not 1–Sal 1 fragment from the 3′ end of the genomic clone was inserted into the Cla 1 and Xho 1 sites of the targeting vector. This construct deleted 132 codons, including the ATG start site in exon 1 of MEKK1, and inserted the neo-resistance gene and polyadenylation signal in the antisense orientation. The linearized construct was introduced into CCE ES cells by electroporation. G418-resistant ES cells were screened for homologous recombination by Southern (DNA) blotting. The frequency of homologous recombination was ~1 in 70. For the generation of MEKK1$^{-/-}$ ES cells, the MEKK1$^{+/-}$ clones were grown at increasing concentrations of G418 up to 10 mg/ml. Two feeder cell–independent CCE MEKK1$^{-/-}$ clones were used for analysis.
13. T. Yujiri, S. Sather, G. R. Fanger, G. L. Johnson, data not shown.
14. JNK activity was assayed by solid-phase kinase assay with GST-c-Jun$_{1-79}$ (GST-Jun) bound to glutathione-Sepharose beads [M. Hibi, A. Lin, T. Smeal, A. Minden, M. Karin, *Genes Dev.* **7**, 2135 (1993)]. The GST-Jun bead assay was verified by JNK immunoprecipitation and in vitro kinase assay with GST-Jun as substrate.
15. MEKK1 was immunoprecipitated from cell lysates with rabbit antiserum to recombinant MEKK1 sequences (*11*). The immunoprecipitates were used in in vitro kinase assays with kinase-inactive MKK4.
16. I. Sanchez, *et al*., *Nature* **372**, 794 (1998).
17. ERK 2 was immunoprecipitated from cell lysates with the C-14 antibody (Santa Cruz Biotechnology, Santa Cruz, CA). Myelin basic protein was used as substrate in in vitro kinase assays [S. J. Cook and F. McCormick *Science* **262**, 1069 (1993)]. p38 was immunoprecipitated with a rabbit antiserum to the COOH-terminus of the kinase, and in vitro kinase assays were conducted with recombinant ATF-2 as substrate [P. Gerwins, J. L. Blank, G. L. Johnson, *J. Biol. Chem.* **272**, 8288 (1997)].
18. I. Herskowitz, *Cell* **80**, 187 (1995).
19. F. Posas and H. Saito, *Science* **276**, 1702 (1997).
20. T. Schlesinger and G. L. Johnson, in preparation.

21. We thank S. Webb and G. Keller for help with ES cell culture. Supported by NIH grants DK37871 and GM30324.

1 May 1998; accepted 3 November 1998

Mutation-Specific Functional Impairments in Distinct Tau Isoforms of Hereditary FTDP-17

Ming Hong, Victoria Zhukareva, Vanessa Vogelsberg-Ragaglia, Zbigniew Wszolek, Lee Reed, Bruce I. Miller, Dan H. Geschwind, Thomas D. Bird, Daniel McKeel, Alison Goate, John C. Morris, Kirk C. Wilhelmsen, Gerard D. Schellenberg, John Q. Trojanowski, Virginia M.-Y. Lee*

Tau proteins aggregate as cytoplasmic inclusions in a number of neurodegenerative diseases, including Alzheimer's disease and hereditary frontotemporal dementia and parkinsonism linked to chromosome 17 (FTDP-17). Over 10 exonic and intronic mutations in the *tau* gene have been identified in about 20 FTDP-17 families. Analyses of soluble and insoluble tau proteins from brains of FTDP-17 patients indicated that different pathogenic mutations differentially altered distinct biochemical properties and stoichiometry of brain tau isoforms. Functional assays of recombinant tau proteins with different FTDP-17 missense mutations implicated all but one of these mutations in disease pathogenesis by reducing the ability of tau to bind microtubules and promote microtubule assembly.

FTDP-17 comprises a group of hereditary neurodegenerative syndromes with diverse but overlapping clinical and neuropathological features (*1, 2*). The signature lesions of FTDP-17 brains are insoluble filamentous aggregates of hyperphosphorylated tau proteins

Table 1. Summary of MT binding and MT assembly promoting properties of WT and mutant tau. AU, absorbance unit.

	MT binding		MT assembly promotion		
	B_{max} (μM)†	K_d (μM)†	Lag time (min)	Initiation rate (AU/min)	A_{350} max†
WT	1.238 ± 0.042	0.039 ± 0.006	2	0.15	0.533 ± 0.003
N279K	1.265 ± 0.055	0.056 ± 0.012	2	0.16	0.538 ± 0.005
P301L	0.883 ± 0.047**	0.079 ± 0.016*	5	0.14	0.522 ± 0.005
V337M	0.909 ± 0.037**	0.048 ± 0.009	3	0.13	0.482 ± 0.005*
R406W	0.628 ± 0.033**	0.089 ± 0.021*	5	0.04	0.406 ± 0.012**

†Mean ± SEM. *$P < 0.05$, **$P < 0.01$.